

See discussions, stats, and author profiles for this publication at: <https://www.researchgate.net/publication/334328728>

Connecting fluvial levee deposition to flood-basin hydrology

Article in *Journal of Geophysical Research: Earth Surface* · July 2019

DOI: 10.1029/2019JF005014

CITATIONS

0

READS

101

3 authors, including:



Scott David

University of Massachusetts Amherst

10 PUBLICATIONS 11 CITATIONS

[SEE PROFILE](#)



Douglas A Edmonds

Indiana University Bloomington

89 PUBLICATIONS 1,305 CITATIONS

[SEE PROFILE](#)

Some of the authors of this publication are also working on these related projects:



Project Bio-morphological modeling Framework [View project](#)

RESEARCH ARTICLE

10.1029/2019JF005014

Key Points:

- Empirical analyses of LiDAR data on the Muscatatuck River, Indiana, USA, show that levee size and shape are unrelated to channel planform
- Numerical modeling reveals that levee initiation is related to the channel planform but subsequent growth is influenced by inundation dynamics in the flood basin
- On tall levees, the levee toe grows faster than the levee crest because it is inundated more frequently, and this causes levees to prograde down-valley over time

Correspondence to:

D. A. Edmonds,
edmondsd@indiana.edu

Citation:

Johnston, G. H., David, S. R., & Edmonds, D. A. (2019). Connecting fluvial levee deposition to flood-basin hydrology. *Journal of Geophysical Research: Earth Surface*, 124.

<https://doi.org/10.1029/2019JF005014>

Received 23 JAN 2019

Accepted 28 JUN 2019

Accepted article online 9 JUL 2019

Connecting Fluvial Levee Deposition to Flood-Basin Hydrology

G. H. Johnston¹ , S. R. David^{1,2} , and D. A. Edmonds¹ 

¹Department of Earth and Atmospheric Sciences, Indiana University, Bloomington, IN, USA, ²Department of Geosciences, University of Massachusetts Amherst, Amherst, MA, USA

Abstract Levees are commonly found along every kind of river system, yet there are no widely accepted models for where along the channel they form and what controls their shape. In this study, we investigated whether levee growth is driven by sediment transfer from the channel adjacent to the levee or by inundation dynamics in the flood basin. To test these ideas, we conducted empirical analyses and numerical modeling of levees on the fine-grained, meandering Muscatatuck River, IN. Using LiDAR data, we found no statistical relationship between the levee and the adjacent channel planform, which suggests levees are not genetically related to their adjacent channel. On the contrary, modeling experiments of a simplified Muscatatuck River show that levee initiation can be genetically related to the adjacent channel because bed shear stress on the floodplain is low where channel curvature is high. But after levees initiate, the genetic connection to the adjacent channel is obscured because levee shape is modified by inundation dynamics. For instance, tall mature levees are not inundated regularly and instead obstruct floodplain flow, creating flow shadows on the downstream side. Sediment is preferentially deposited in the flow shadow, which moves the location of maximum deposition from the levee crest to the toe. This causes levees to prograde down-valley, which reshapes the levee and genetically disconnects it from the channel. We propose that this morphodynamic mechanism of levee growth is characteristic of fine-grained rivers in narrow floodplains where flood basins can act as conveyance channels that transport sediment down-valley before deposition.

1. Introduction

Fluvial levees are sedimentary deposits elevated above the surrounding floodplain that form near the bank of a river. Because they are elevated and positioned along the bank, they influence flooding patterns, and the bidirectional exchange of water, sediment, and pollutants between the channel and floodplain (Adams et al., 2004; Brierley et al., 1997; Nanson & Croke, 1992). This, in turn, affects soil development, agricultural activity, and hazards to population centers within the flood basin (Brakenridge et al., 2017; Wolfert et al., 2002). Levees also influence fluvial stratigraphy because as they grow, the potential for avulsion increases as the water surface becomes elevated above the floodplain (Bryant et al., 1995; Mackey & Bridge, 1995; Mohrig et al., 2000). Due to their stratigraphic architecture, levee deposits are often targeted for hydrocarbons (Fielding & Crane, 1987). Despite the societal and scientific importance of levees, we do not know what sets their presence, size, and shape.

Our current understanding of levee deposition is surprisingly cursory—empirical studies thus far have not revealed consistent controls on levee presence, size, or shape. Levees are thought to occur along both banks of a river, but on some meandering rivers they are more pronounced along the cut bank where they are not disturbed by scroll bar formation (Brooks, 2005; Hudson & Heitmuller, 2003; Kesel et al., 1974). However, in other cases, levees show little preference and occur on most river banks (Smith et al., 1989), only on straight reaches (Ferguson & Brierley, 1999), or on alternating sides (Iseya & Ikeda, 1989). Similarly, during flood, more deposition tends to occur on shorter levees, but there is no clear control on the magnitude of deposition (Smith et al., 2009). There is some field evidence that vegetation influences levee occurrence (Vargas-Luna et al., 2018) and shape (Pierik et al., 2017), but in these cases it is hard to isolate the cause and effect. Levee shape should also be related to the dominant grain size, because all else being equal, channels with fine-grained sediment should produce wide levees, but the relationship is often ambiguous (Adams et al., 2004). These empirical studies show no consistent results probably because we still do not know the basic conditions for levee formation, making it hard to isolate controls on levee shape.

Levees form when sediment is deposited in a zone of reduced flow competence along the channel margins. A reasonable starting assumption is that the levee is genetically related to the adjacent channel, which would occur if levees form when sediment-laden flood water is decanted over the bank and sediment is immediately deposited (Aalto et al., 2003). In this case, the local channel and sediment characteristics—planform, depth, width, hydrology, and grain settling—govern movement of sediment to the margins where levees form. This notion is encapsulated in early models: assuming a straight channel, it can be shown that suspended sediment is transferred to the channel margin by fluid advection and turbulent eddy diffusion (Adams et al., 2004; James, 1985; Marriott, 1992; Mertes, 1997; Nezu & Nakagawa, 1993; Pizzuto, 1987; Pizzuto et al., 2008; Shiono & Knight, 1991). These studies promote the idea that the levee is genetically related to the adjacent channel segment, even though field data are equivocal and show no consistent relationship between the levee and any measure of the adjacent channel.

On the other hand, levees may not be genetically related to the adjacent channel, especially if levee sediment is not locally decanted from the channel but instead originates from sediment-laden floodwaters moving down-valley. This implies that flood basins are more than just water storage locations—they convey water and sediment long distances, sculpting levees in the process (Filgueira-Rivera et al., 2007; Pierik et al., 2017). Consistent with this are observations that floodplain sedimentation patterns depend on flood wave movement, inundation time, magnitude, and the presence of perirheic zones (Asselman & Middelkoop, 1995; David et al., 2017; Mertes, 1997; Middelkoop & Van der Perk, 1998; Nicholas & Mitchell, 2003; Walling & He, 1998). One interesting example shows that levee deposition occurs even when water in the adjacent channel does not overtop the levee. Filgueira-Rivera et al. (2007) demonstrate that the levee crest and toe can grow quasi-independently because the toe is at a lower elevation and is inundated by sediment-laden water more frequently. This suggests levee deposition may not be related to the adjacent channel but instead occurs as the flood wave transports fine-grained sediment down-valley to positions behind fluvial levees on the floodplain. If this process dominates, then levee form may be dictated by flood-basin hydrology and sediment transport during flood rather than the detailed mechanisms of sediment transfer from the adjacent channel to the margin.

The focus of this paper is to assess whether levee presence and geometry are genetically related to the adjacent channel or to flood-basin hydrology. We assess this by measuring and modeling levee presence, size, and shape on the meandering Muscatatuck River, Indiana, USA. We have two hypotheses for how levee deposition should be connected to the adjacent channel in meandering rivers. Our first hypothesis is that levee heights and widths should scale with curvature because curvature drives superelevation of the water surface and promotes advective sediment transport across cut banks (Ervine et al., 1993; Ervine et al., 2000). Our second hypothesis is that levees should be most prevalent and largest in the crossover region (i.e., where the channel centerline is perpendicular to the floodplain centerline) because this is where advective transport of channel sediment into the floodplain is maximized (Czuba et al., 2019; Ervine et al., 2000; Shiono & Muto, 1998). Our alternative to these two hypotheses is that levee formation is not related to the adjacent channel and instead dictated by flood-basin hydrology. To test these hypotheses, we conducted an empirical analysis of near-channel topography along the Muscatatuck River, IN, and its association with the adjacent channel curvature and orientation relative to the floodplain centerline. Assessing the role of the flood basin in the empirical data is problematic without detailed records of flood wave propagation, inundation patterns, and historical flooding. To circumvent this, we assess the role of the flood basin with numerical modeling. Based on our numerical modeling, we show how levee deposition can occur independently of the adjacent channel and how levee formation in this scenario is ultimately governed by flood-basin hydrology. In both the empirical data and the modeling experiments, we neglect the influence of vegetation on levee formation, even though it can be important (Pierik et al., 2017), because we cannot isolate its effect given that all but 500 m of the reaches in our study are vegetated.

2. Field Study Site

Our field study focuses on the Muscatatuck River (Figure 1), which flows westward from the Muscatatuck Plateau across the Scottsburg Lowlands through southern Indiana (USA) eventually meeting the East Fork of the White River to the west. The Scottsburg Lowlands run approximately north-south between the Muscatatuck Plateau to the east and the Norman Upland to the west. This region lies south of the

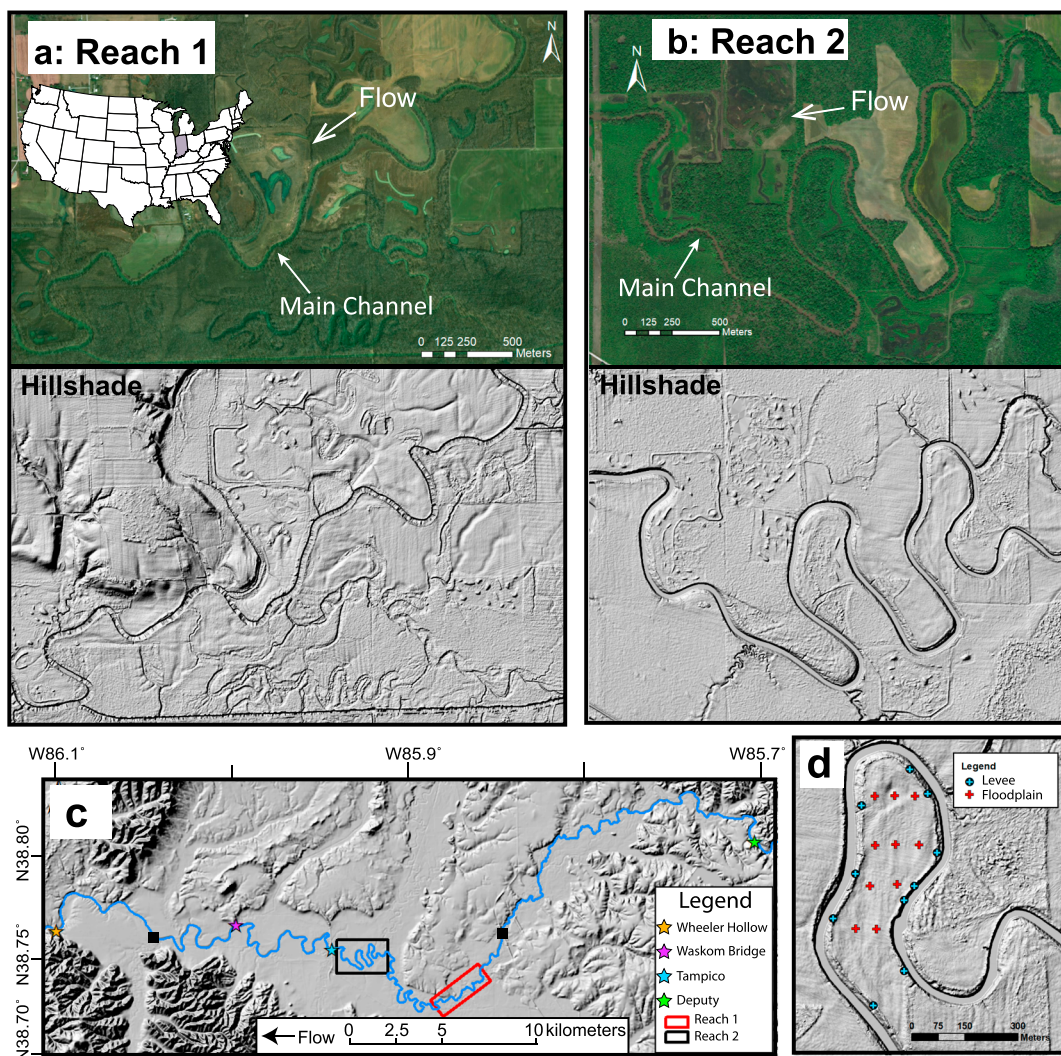


Figure 1. (a and b) Satellite and hillshade images, generated from 1.5-m resolution elevation data, for Reaches 1 and 2 along the Muscatatuck River, Indiana. Flow direction in the main channel is indicated on the satellite imagery. Channel bathymetry is from hydro-flattening created to insure a hydrologically correct elevation model. (c) Longer reach showing the locations of Reaches 1 and 2 (boxes), and locations of river-spanning bridges where suspended sediment samples were collected (stars). These are also locations of United States Geological Survey gauges used for data in Figure 2. Black squares mark the beginning and end of the reach of the Muscatatuck River analyzed in radius of curvature analysis in Figure 9. (d) Sediment sample locations along Reach 2. Inset map in (a) shows location of Indiana, USA.

Wisconsin Glaciation boundary and may have served as a conduit for glacial outwash flowing south to the Ohio River. Underlying this physiographic region is Devonian and Mississippian age limestones, shales, and siltstones. Across this area, the Muscatatuck River continues to incise into sediments weathered from the underlying New Albany Shale to the east and the Borden Group shales to the west. The Muscatatuck River incision into this easily eroded, fine-grained siltstone and shale accounts for the fine-grained sediment load. From the downstream most point in our study area the Muscatatuck drains 2,950 km².

We selected two reaches along the Muscatatuck River for detailed analysis of the near-channel topography (Figures 1a and 1b). We refer to the topography as near-channel because not all reaches contain levees. These reaches were chosen because both are prone to frequent flood events that fully inundate the surrounding floodplains, and both have levees along the channel margins. Also, neither of the reaches are lined with anthropogenic flood control structures, such as dikes or dams, or elevated road beds, which would obscure natural features. Both reaches flow through low gradient, agricultural land in southern Indiana.

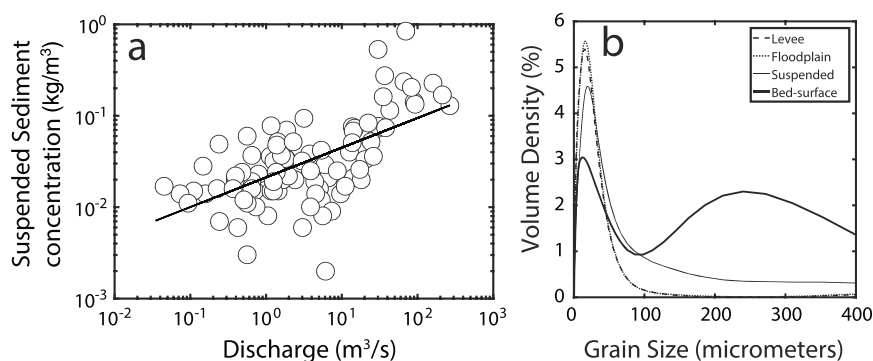


Figure 2. (a) Suspended sediment rating curve for the Muscatatuck River from United States Geological Survey suspended sediment concentration samples collected at the Deputy, Indiana, gauge station. (b) Channel bed surface distribution is the average of four samples collected near Waskom and Wheeler Hollow bridges, and suspended sediment distribution is the average of 51 samples collected at Deputy and Wheeler Hollow. Floodplain and levee crest grain size distributions are the averages of 10 samples collected along Reach 2. In all cases, sample locations are shown in Figures 1c and 1d.

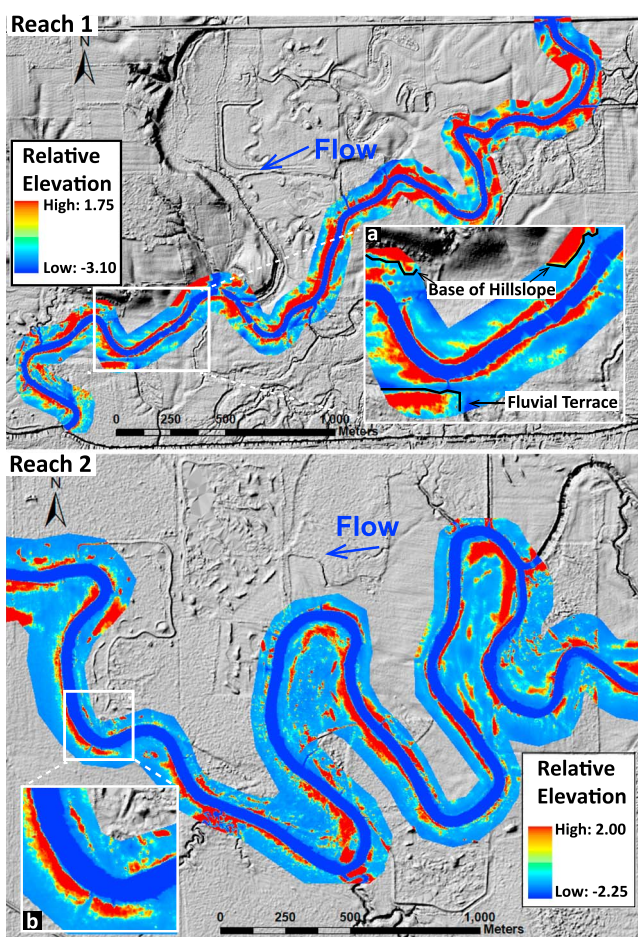


Figure 3. Histogram equalization and detrending visualization methods for near-channel topography along Reaches 1 and 2 of the Muscatatuck River. Elevation is measured relative to the detrended floodplain surface.

3. Methods

3.1. Morphology, Hydrology, and Sedimentology of the Muscatatuck River

We analyzed near-channel topography using a 1.5-m resolution, bare-earth digital elevation model (DEM), derived from statewide Light Detection and Ranging (LiDAR) data. The LiDAR data set was collected by a nonprofit consortium during the statewide campaign to collect high-resolution LiDAR and orthophotography data from 2011 to 2013 (www.indianamap.org). The bare-earth DEM was created by finding the last return for each laser pulse, which is typically the bare-earth return, and averaging all bare-earth returns within 1.5-m × 1.5-m bins. More information about the vegetation removal is provided in the LiDAR metadata through the state of Indiana. Reach 1 has a channel centerline distance of 5,210 m, the average channel width is 28 m, and the sinuosity—measured as the channel centerline distance divided by the upstream to downstream straight-line distance—is 1.78 (Figure 1a). Reach 2 is located approximately 8.9 km downstream from Reach 1 and has a channel centerline distance of 7,557 m, the average channel width is approximately 32 m, and the sinuosity is 3.04 (Figure 1b). The floodplain valley width for both Reaches 1 and 2 ranges from 3 to 8 km. The floodplain slopes for Reaches 1 and 2 are 0.00033 and 0.00027, respectively; the channel bed slopes for Reaches 1 and 2 are 0.00021 and 0.00011, respectively. The average bankfull depth through both reaches of the Muscatatuck River measured from a single-beam echo sounder is approximately 2 m.

To characterize the suspended sediment concentrations in the Muscatatuck River, we collected 51 suspended sediment samples and augmented these data with 90 suspended sediment concentration samples collected by the United States Geological Survey (USGS) at the stream gage (03366500) in Deputy, Indiana (Figure 1c). Sediment data were accessed through USGS Sediment Data Portal. We collected suspended sediment samples from four bridges spanning the Muscatatuck River (denoted by stars in Figure 1c) on 7 February 2015, 4 and 11 March 2015, 12 April 2015, and 21 January 2017 during bankfull to flood stage discharge (20–198 m³/s) according to USGS standard operating

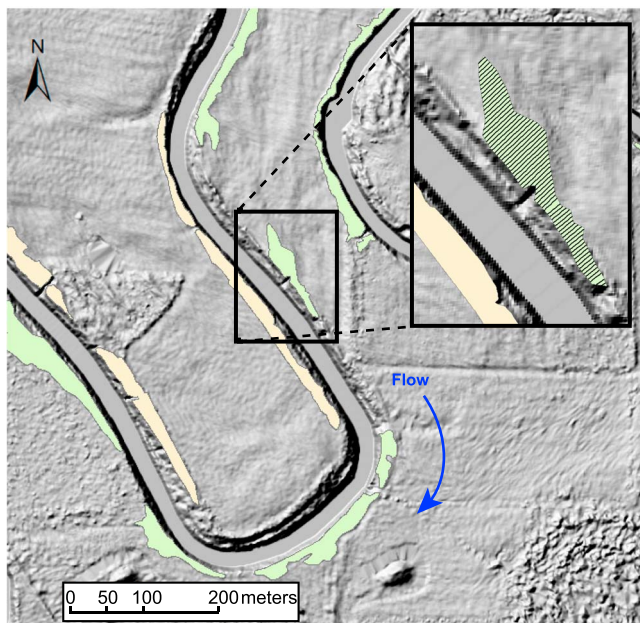


Figure 4. Examples of closed-contour polygons showing the spatial extent of the levee deposits determined from levee toe contour elevation. The levee widths and height values were extracted for each levee polygon. Levee width is measure along channel-perpendicular transects clipped to the levee polygon extent, as shown in inset box. Colors indicate river right or river left side.

procedures using a US-DH59 sampler (Edwards et al., 1999). Suspended sediment concentrations were measured with the evaporation method procedures laid out in the ASTM International Test Method, D 3977–97(B).

To characterize the grain size in the channel and floodplain, we collected four channel-bed-surface sediment samples during bankfull to flood-stage flow, and 10 hand auger samples from the levee and 10 from the floodplain. Channel-bed-surface samples were collected from the Waskom and Wheeler Hollow bridges (Figure 1c) on 20 January 2016 using a Ponar® grab sampler according to standard operating procedures laid out by the U.S. Environmental Protection Agency (Simmons, 2014). Levee and floodplain deposits were sampled at Reach 2 using a hand auger (Figure 1d). Two replicate samples were collected at each location, and samples for analysis were taken 0.75 m below the surface to avoid sampling organic root material or surface soil that may have been modified by agricultural activities. Grain size was measured with a Malvern Mastersizer® 3000E.

The Muscatatuck River is silt dominated with moderate to high suspended sediment concentrations. Combining our samples and ones from USGS, the average suspended sediment concentration during bankfull flow ($Q = 35 \text{ m}^3/\text{s}$) or higher for the Muscatatuck River is 0.23 kg/m^3 (Figure 2a). The median grain size for suspended and bed-surface sediment was 15.7 and $27.7 \mu\text{m}$, respectively. Median grain size for the levee and floodplain deposits were 9.8 and $10.1 \mu\text{m}$, respectively (Figure 2b). There was no systematic difference in the channel-bed grain size across the four measurement locations.

3.2. Quantifying Near-Channel Topography

Quantifying near-channel topography is a deceptively challenging task. Idealized levee shapes are conceptually simple—most models depict levees as gull wing-shaped deposits with elevations that exponentially taper from a maximum at the crest out to the levee toe (Hudson & Heitmuller, 2003). But natural levees rarely follow this shape and instead show a wide variability of shape and orientation relative to the channel margin. This variability and complexity are harder to capture when levee geometry is measured with coarsely spaced cross-sections perpendicular to the channel centerline.

The methodology we have developed captures the full two-dimensional planform shape of the levee. We first detrended the DEM by removing the average floodplain slope from the topography. The average floodplain slope was derived from a triangulated irregular network (TIN). The TIN surface was computed by sampling elevations along evenly spaced cross-sections down the floodplain. The resulting TIN surface maintained all long wavelength topography and removed all short wavelength topography. We found that using this surface to remove down-valley slope minimized distortion of small-scale features when detrending the floodplain. Next, we isolate near-channel topography in the LiDAR data within three channel widths along both banks using a histogram equalization method. This method is often used by the medical industry to analyze X-rays because the data distribution is reshaped to create a linear cumulative distribution function, which has the distinct advantage of enhancing low contrast areas (Hum et al., 2014). In the context of a DEM, this enhances the low relief of the levee toe where slopes are small (Figure 3).

Using the histogram equalized image, we then picked an elevation value for the levee toe by inspecting cross-sections. Like previous researchers, we identified the levee toe on different cross-sections as the location where the levee slope decreases to approximately 0.01 m/m (Cazanacli & Smith, 1998; Filgueira-Rivera et al., 2007). In areas where levee deposits abut more complex topographic surfaces, we determined the levee toe by defining the first major break in topography after the levee crest (Adams et al., 2004). Otherwise, the levee toe was delineated from changes in land use or vegetation (Hudson & Heitmuller, 2003) identified as the boundary between riparian vegetation and farmland. The levee toe contour elevation was determined by

Table 1
Model Parameters for Delft3d Simulation

Hydrodynamic parameters		
Water density	1,000	kg/m ³
Horizontal eddy viscosity	0.001	m ² /s
Horizontal eddy diffusivity	1	m ² /s
3-D turbulence model ^a	$\kappa-\epsilon$	—
Manning roughness	0.035	—
Sediment parameters		
Settling velocity	0.23	mm/s
Specific density	2650	kg/m ³
Dry bed density	1350	kg/m ³
Density for hindered settling	1600	kg/m ³
τ -crit for sedimentation ^b	0.5	N/m ²
τ -crit for erosion ^c	2	N/m ²
Erosion parameter	0.0001	kg/m ² /s
Initial sediment layer	0.5	m
Morphological scaling factor	70	—

^aKappa-Epsilon ($\kappa-\epsilon$) 3-dimensional turbulence closure model. ^bCritical shear stress for sedimentation. ^cCritical shear stress for erosion.

thorough inspection of individual cross-sections and analysis of satellite and hillshade imagery. We avoided any anthropogenic features, such as elevated road beds or drainage ditches. Additionally, natural features not genetically related to the channel, such as fluvial terraces and continuous low angle hillslopes, were excluded from the levee analysis (inset a, Figure 3).

We then defined individual levee polygons from closed contours at the elevation of the levee toe (Figure 4). Closed contours define a single levee, and in some cases, these are defined depositionally, but in other cases they are defined erosional as when channels cut through the levees (inset b, Figure 3). Levee width for each polygon was determined by calculating channel-perpendicular transects, spaced 2 m apart, and clipping them at levee polygon boundaries (Figure 4, inset). Average levee width is calculated as an arithmetic mean of all cross-sections within a given polygon on each channel bank. Levee height values were extracted as the highest value for each channel-perpendicular transect and then averaged across all transects. Local channel centerline curvature was measured using RivMAP (Schwenk et al., 2017). We also calculate the radius of curvature by fitting a circular arc to the channel centerline using satellite imagery available through Google Earth Pro®. The channel centerline was defined as the midpoint between the cut bank and the inside point bar.

Finally, we calculated the orientation of levee deposits relative to the floodplain centerline. The levee and floodplain centerlines were determined with Thiessen polygons. We grew two sets of Thiessen polygons, one from the boundaries of the levee and one from the boundaries of the floodplain polygons. The levee polygons were defined by the levee toe contours, and the floodplain polygon was defined by floodplain terrace boundaries. For each set of Thiessen polygons, the line where they meet was taken as the levee and floodplain centerlines (David et al., 2017). Then the angle between the two centerlines was measured as the difference between the azimuth orientation of each centerline measured in degrees.

3.3. Numerical Modeling Methods

3.3.1. Flow Modeling in Delft3D

We conducted numerical modeling experiments using Delft3D, which solves the coupled 3-D fluid flow field and bed evolution (i.e., the Navier-Stokes equations). For 3-D flow, Delft3D solves the shallow-water equations with a user specified number of depth layers. In this paper we used eight layers with thicknesses decreasing in thickness from the water surface to the bed. The vertical transport of momentum between the flow layers is accounted for using the kappa-epsilon turbulence closure model. The model solves for the 3-D transport of sediment by calculating the advection and diffusion of suspended particles using the flow velocity terms and the eddy diffusivities derived using the Navier-Stokes equations.

3.3.2. Model Domain Selection

To explore controls on levee depositional patterns, we choose a model domain covering a channel reach with several meander bends that allowed for an examination of the hydrodynamic conditions during flood events. We selected Reach 2 for this analysis (Figure 1b) because it contains multiple river meander bends, and we observed the presence of levees along the channel in LiDAR data. The modeling domain covers a floodplain area that is 2,500 m long by 1,700 m wide. Our model domain is the same extent as shown in Figure 1b. In the model we retained the shape of the river in planform but synthetically flattened the floodplain topography so we could easily assess how the flood wave interacts with the channel during flood. This effectively assumes that the levees were

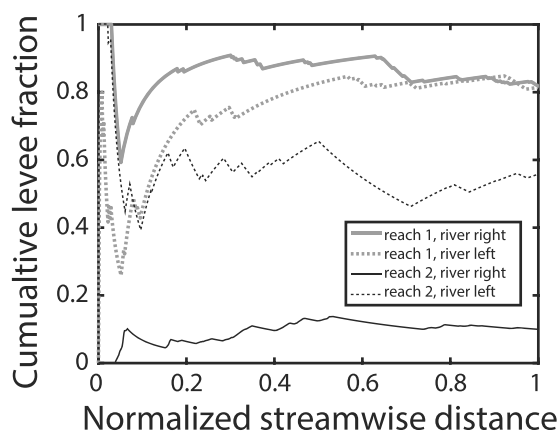


Figure 5. Levee presence along Reaches 1 and 2. Cumulative levee fraction is the total linear distance of levee measured from zero to each normalized streamwise distance and then nondimensionalized by the total length. For example, from 0 to the normalized streamwise distance of 0.2, Reach 2 (river right) has levees on ~5% of the bank. Increases and decreases in normalized levee length, respectively, represent leveed and unveeded parts of the reach. Streamwise distance is normalized by the total length. Value at normalized streamwise distance of 1 indicates fraction of entire reach covered by levees.

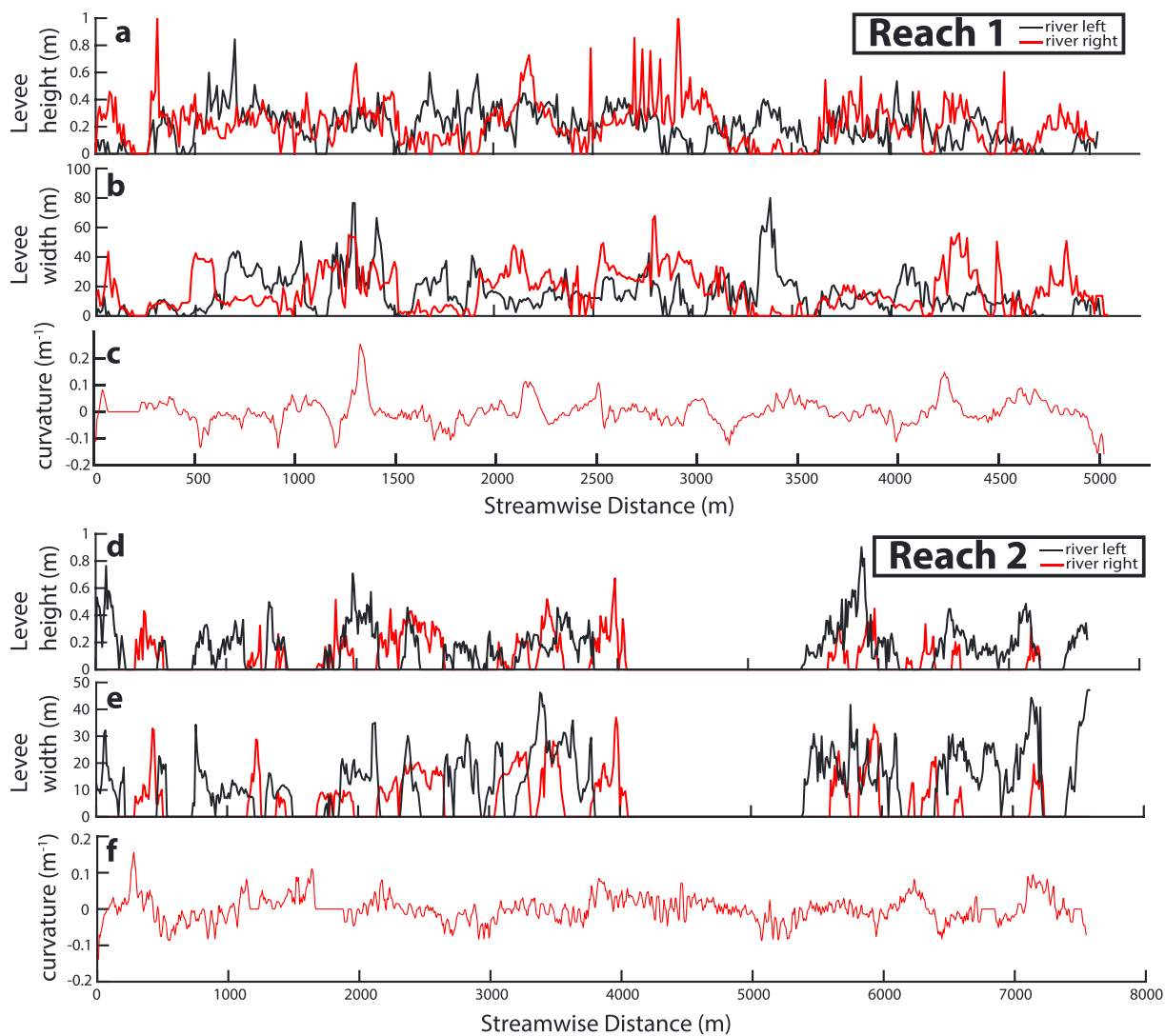


Figure 6. For both reaches, levee height (a and d) and width (b and e) are shown for every 2-m channel-perpendicular cross-section (see example in Figure 4). Curvature (c and f) is calculated from the channel centerline following Schwenk et al. (2017).

formed in a land use setting like today. The smoothed floodplain has a slope of ~ 0.00027 m/m and channel slope of ~ 0.00011 m/m, consistent with field observations. The channel was 2 m deep, consistent with field measurements, and with a rectangular cross-sectional shape. A random centimeter-scale topographic perturbation was also added across the model domain to the surface to allow for more realistic flow propagation. We added a straight channel segment at the upstream boundary of the model for flow establishment prior to entering the first meander bend. We also smoothed the channel bankline boundaries to encourage a more natural flow condition and minimize grid effects.

3.3.3. Boundary Conditions and Physical Parameters

Flow enters the domain along the eastern boundary and exits to the west. The upstream boundary was set across the channel width at the eastern boundary and defined the time-dependent fluid discharge entering the domain. The downstream boundary was a time-varying water level elevation that was chosen to prevent backwater or drawdown effects based on the upstream discharge. The north and south model boundaries were defined as Neumann boundaries, which allows fluid and sediment to smoothly exit or enter the boundary. At the upstream boundary, the incoming sediment flux was set to a constant 0.23 kg/m^3 with a density of $2,650 \text{ kg/m}^3$ and a grain size of 0.016 mm . These values are consistent with observations (Figure 2). This size was determined based on the median grain size of suspended sediment sampled during field operations. The settling rate of grains is 0.23 mm/s (Ferguson & Church, 2004). Additional modeling parameters are reported in Table 1.

Table 2
Levee Statistics on Reaches 1 and 2 of the Muscatatuck River

	Median height (m)	Range in levee height (m)	Median width (m)	Range in levee width (m)
Reach 1, river left	0.21	0.05–0.84	16.9	0.6–30.7
Reach 1, river right	0.19	0.08–1.1	13.8	0.6–36.2
Reach 2, river left	0.20	0.04–0.9	21.9	4.2–16.1
Reach 2, river right	0.17	0.07–0.7	16.1	6.3–38.8

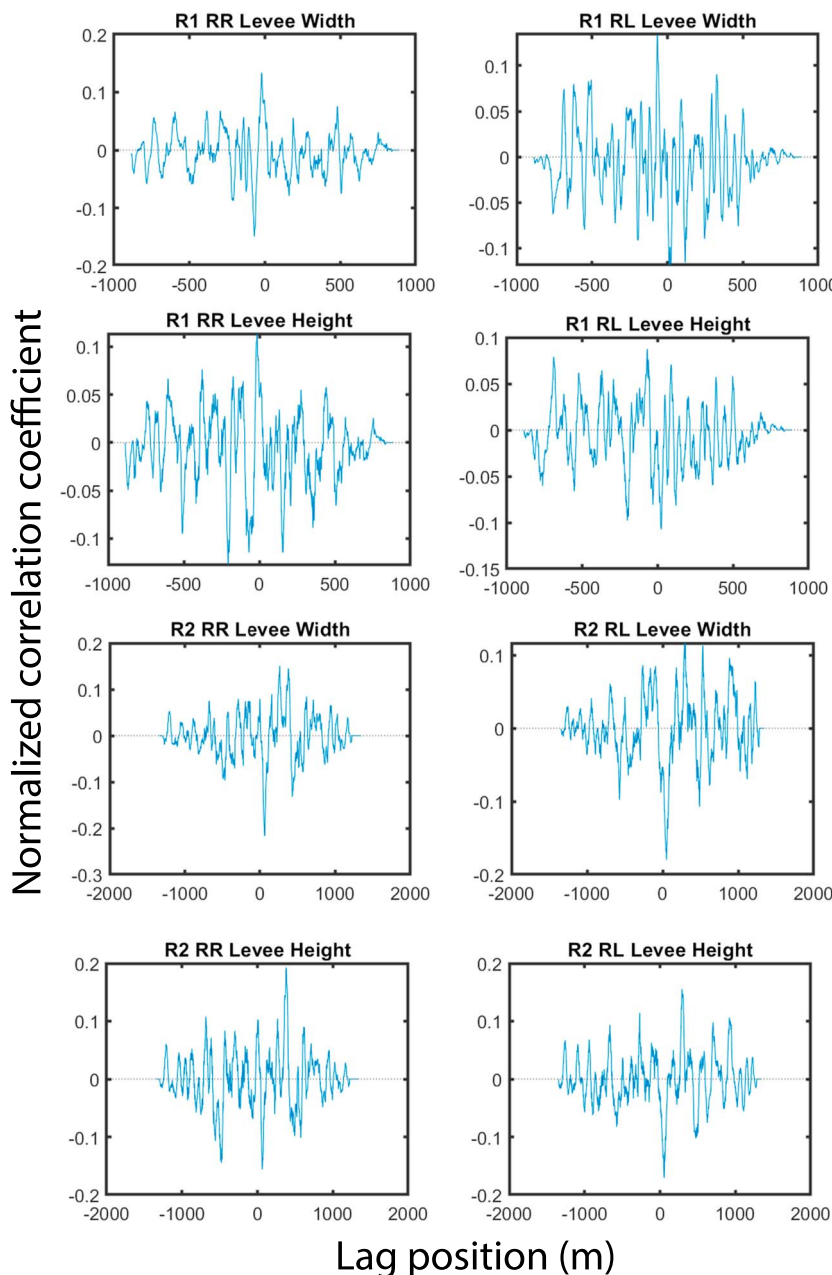


Figure 7. Cross-correlation function between channel curvature and levee height and width (data shown in Figure 6). Cross-correlation measures the similarity between curvature and levee height or width for different shifted (lagged) copies of curvature. R1 = Reach 1; R2 = Reach 2; RR = River Right; RL = River Left.

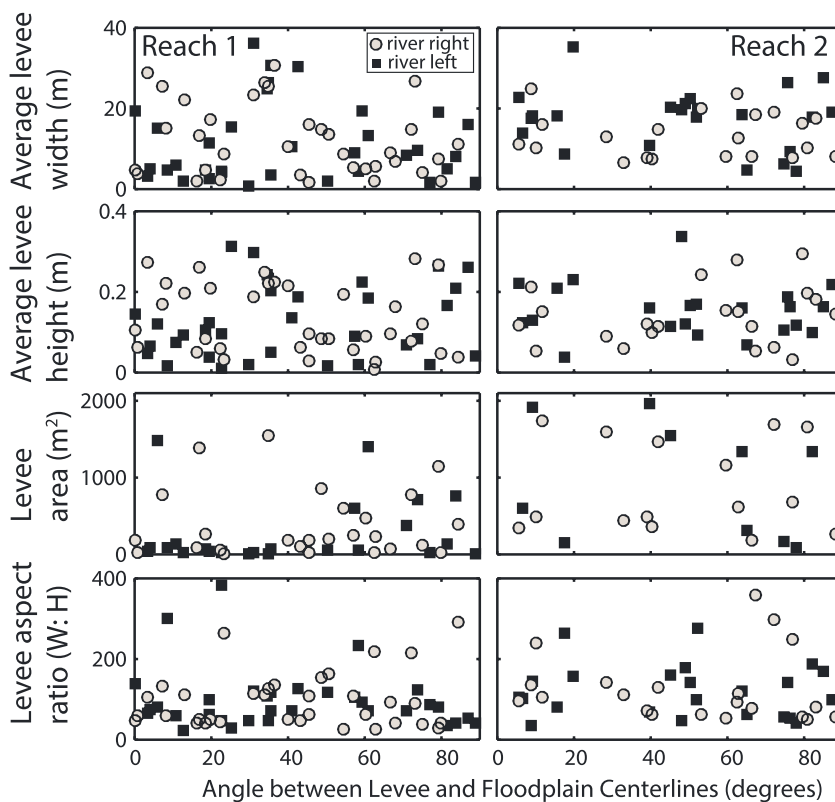


Figure 8. Levee morphometrics plotted against relative orientation for Reaches 1 and 2 along the Muscatatuck River. Relative orientation (in degrees) is the angle between the centerline of the levee and floodplain. Zero indicates the long axis of the levee is parallel to the floodplain centerline. Data are average values for each closed-contour levee polygon (see example in Figure 4). See Figures 1a and 1b for location of these reaches.

The primary factors that drive suspended sediment deposition and erosion within the modeling domain are the critical shear stress for sedimentation and erosion. There are numerous factors, such as vegetation, microtopographic variations, and grain flocculation, for example, that cause deposition of silt- and clay-sized grains on the floodplain. Our model was not able to account for all these factors. To allow for deposition of sediment during a flood event, we set the critical shear stress for sedimentation at 0.5 N/m^2 , consistent with experimental studies of mud deposition (Maa et al., 2008). This value permits a reasonable amount of deposition in the domain. The critical shear stress for erosion is set to 2 N/m^2 , which also falls within the reasonable range for erosive shear stresses for fine-grained, cohesive sediment and does not allow for excessive channel erosion during elevated discharge events (Clark & Wynn, 2007; Kimiaghaham et al., 2016). Based on historical satellite imagery, we know that the Muscatatuck River channel is relatively stable and any shear stress values for erosion that allow for rapid changes to the channel planform are not representative of the natural system. Deposition of fine-grained silt within the model domain occurs slowly, so we used a morphological scaling factor of 70 for these modeling experiments to speed up change. The morphological scaling factor is a commonly used approach that multiplies the sediment fluxes to or from the bed to speed up the changes (Lesser et al., 2004; Ranasinghe et al., 2011; Roelvink, 2006).

3.3.4. Modeling Experiment

To quantify the evolution of levee morphology, we flooded the model domain from the upstream boundary four times with identical triangular flood waves. The flood waves were symmetrical and peaked at $100 \text{ m}^3/\text{s}$. Each flood wave lasted 2 days and started and stopped at a minimum discharge of $10 \text{ m}^3/\text{s}$. The peak discharge completely inundated the floodplain, and floodplain waters exited the domain before the next flood event. The entire four-wave experiment lasted 8 days of model time. It is difficult to scale this time precisely, but the discharge magnitude roughly corresponds to 0.5- to 1-year flood, and given the morphological scale factor of 70, this amount of bed change could represent 140–280 years of actual time.

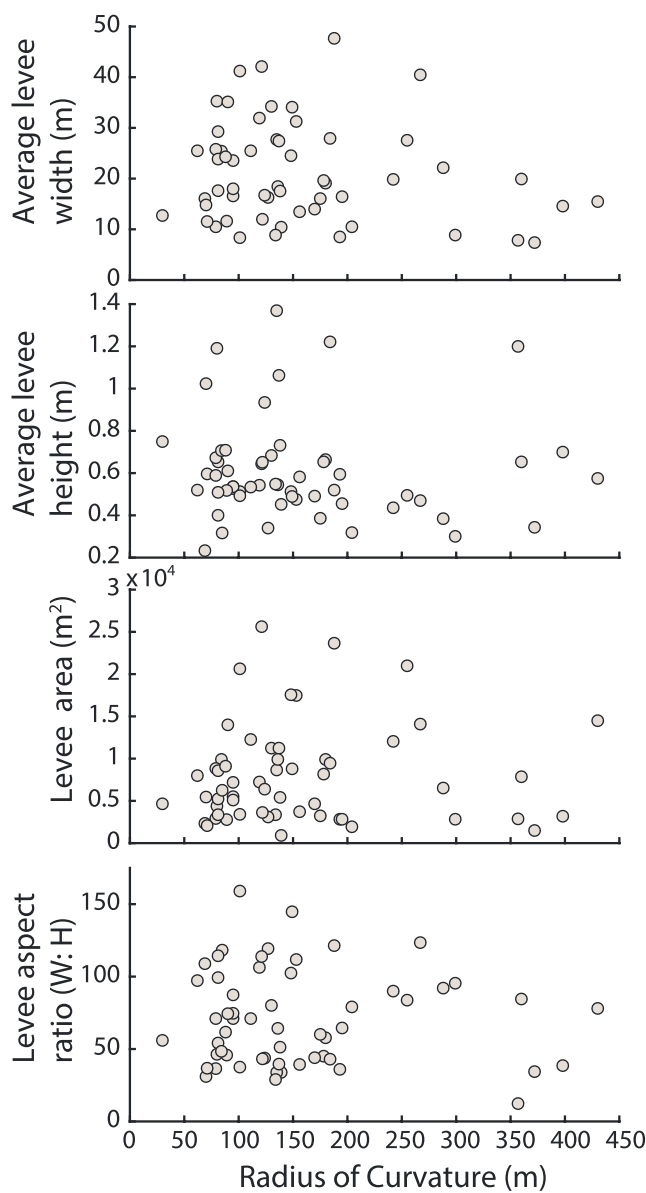


Figure 9. Levee morphometrics plotted against channel radius of curvature for 54 meander bends along the Muscatatuck River. See Figure 1c for location of this reach.

For this analysis, we increased our study reach to 44 km of channel centerline distance to include more meander bends (Figure 1c). For these bends, we only considered cut banks because these levees are not obscured by scroll bars and are easier to identify. We found no relationship between channel radius of curvature and levee morphology (Figure 9). That said, the range of levee width and height decreases with radius of curvatures (Figures 9a and 9b). Aspect ratio and basal area showed a high degree of variability across the range of channel radius of curvature values, and no clear relationships exist (Figures 9c and 9d).

In summary, these empirical data show no clear relationship between the adjacent channel and levee formation. This may instead suggest that levee deposition on the Muscatatuck River is instead governed by flood-basin hydrology. Unfortunately, we cannot test how flood-basin hydrology affects levee formation in our field data because we lack any empirical data on flood wave hydrology for the Muscatatuck River. Because of this, in the following section we conduct generic modeling experiments to test how a fine-grained river system might create levees during overbank flow.

4. Empirical Analysis of Levee Morphology on the Muscatatuck River, Indiana, USA

Based on our definition of levees and methods for their delineation, we mapped the presence of levees along the two reaches of the Muscatatuck River (Figure 5). On Reach 1, levees are more common and occur along 80% of the banks, whereas in Reach 2, levees occur along 55% and 10% of the left and right banks, respectively (Figure 5). Levee presence on river right and river left sides shows some degree of correspondence. On Reach 1, both sides have a decreasing levee presence until normalized stream distance of 0.1 (see Figure 5 for definition of normalized stream distance) and then become progressively more leveed downstream. On Reach 2, both river right and river left have unleveed portions from normalized stream distances of 0.5 to 0.75. This suggests that levees tend to be paired. For a given reach, paired levees show little similarity between their heights and widths at a given position (Figure 6). We find no evidence through regression or series correlation that these series are related, suggesting paired levees are not similar. Median levee heights and widths for both reaches are reported in Table 2.

To explore controls on levee shape, we compared the local channel centerline curvature for both reaches to levee geometry. We calculated the channel curvature as the second derivative of the channel centerline (Schwenk et al., 2017; Figures 6c and 6f). We calculated the cross-correlation between the curvature series and levee width or height to determine whether levee geometry is in phase (plus or minus a lag) with channel planform. We found that levee morphology is not in phase with channel curvature (Figure 7). In some cases, there may be a slight correlation between levee width and channel curvature (e.g., river right levees along Reach 1 at the zero-lag position; Figure 7). However, the value does not rise significantly above the background. These results suggest that variations in the height and width of levees along the Muscatatuck River are unrelated to channel curvature.

For Reaches 1 and 2, we also explored whether levee morphology was determined by the orientation between levee centerline and floodplain centerline (Figure 8). Angle values near 0° mean the levee centerline is parallel with a floodplain centerline, whereas values of 90° mean the levee centerline is perpendicular to the floodplain centerline. There is no obvious relationship between the orientation of the levee relative to the floodplain and all levee variables considered (Figure 8).

We finally explored the relationships between channel radius of curvature and levee geometry for 54 meander bends along the Muscatatuck River.

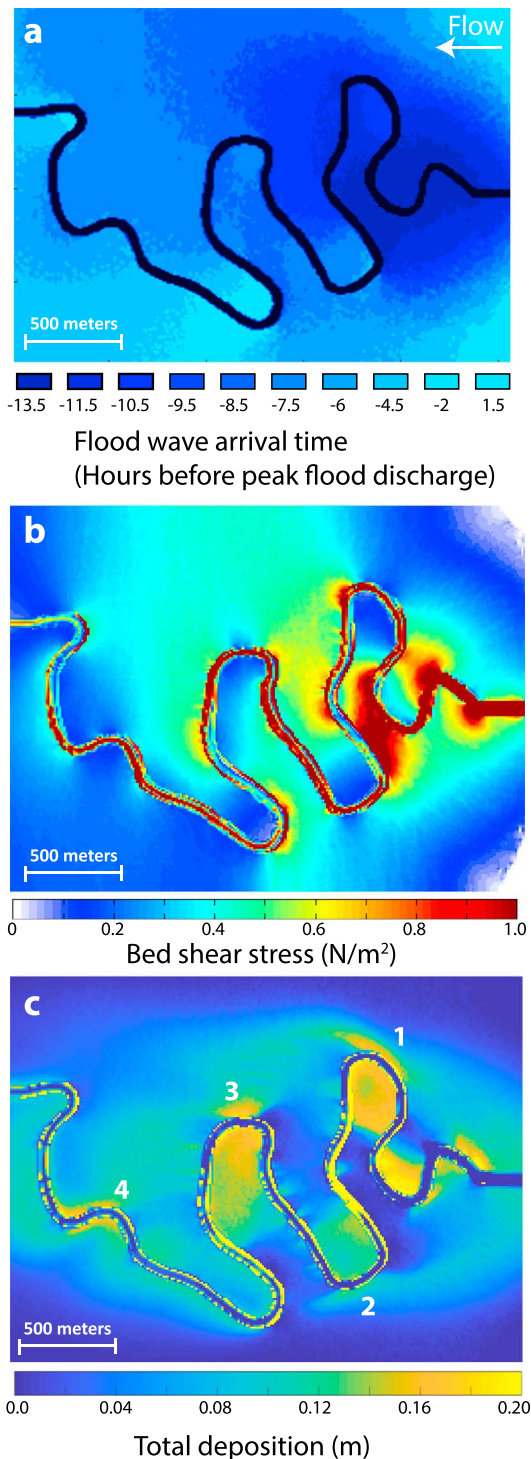


Figure 10. (a) Model results showing flood wave arrival time prior to any morphologic change. Flood wave arrival is defined as inundation greater than 10 cm. The inundation front is noisy because of the random topographic roughness. (b) Modeled bed shear stress at peak discharge prior to any morphodynamic change. (c) Total deposition after the four flood wave experiment. Numbers 1–4 refer to levees analyzed in Figures 11–13.

at Locations 3 and 4 are oriented approximately parallel to the down-valley slope. Temporal evolution of levee shape and size shows that all levees grow down-valley during subsequent flooding events

5. Morphodynamic Modeling of Levee Formation

In this section we use modeling experiments to explore physically plausible explanations for why levee deposition may not be genetically related to the channel and to explore other factors that control levee deposition, like flood-basin hydrology, that are hard to constrain in the field. Because we are focused on understanding cause and effect, we model a simplified version of Reach 2, which retains the channel shape but flattens the topography so that we can more clearly assess the relationship between the channel and flood-basin hydrology. We also ignore the role of vegetation. While vegetation can be important (Pierik et al., 2017), we do not know the vegetation conditions when these levees were formed. Considering this approach, we do not expect modeled levee deposition to perfectly match the field data, and these model results are meant to explore conceptual ideas for levee formation on a river that is like the Muscatatuck.

To explore the processes that lead to levee formation and growth on the Muscatatuck River, we model levee morphodynamics in Delft3D along Reach 2 through four consecutive flood waves. Each flood wave is symmetrical and peaks at 100 m³/s discharge and starts and stops at a minimum of 10 m³/s discharge. Bankfull discharge is achieved at approximately 35 to 40 m³/s. Peak discharge results in complete inundation of the floodplain while still maintaining the high-velocity channelized flow. Floodplain water depth during peak inundation is approximately 0.5 m.

Prior to the morphodynamic simulation, we first simulated the reach with only hydrodynamics. In this case, as the flood wave moves down-valley, there is surprising variability in flood-wave arrival times given the simplicity of the floodplain (Figure 10a). For instance, the southern half of the floodplain inundates a few hours later than the northern half. This is caused by the interaction of the flood with the meandering channel, which serves as a macro roughness element. During peak inundation, there are distinct zones of high and low bed shear stress that emerge because the flood wave interacts with the channel (Figure 10b). Downstream of meander bend apices, the expulsion of high velocity channel waters creates locally high bed shear stress (Sellin et al., 1993; Shiono & Muto, 1998). However, at the apex of the meander bend, channel and floodplain flow are aligned and bed shear stress in this region is low.

During the four flood waves, sediment deposition occurred on the channel margins and across the floodplain (Figure 10c). Levee deposition occurs where the bed shear stress is less than the critical value for sedimentation (0.5 Pa; Table 1) in our experiments (compare Figures 10b and 10c). The thickest levee deposits occur at meander bend apices where channel curvature is highest. As expected, total levee deposit thicknesses are small; typically, on the order of 10 to 20 cm, but they are consistent with field measurements (Table 2; Figure 6). The locations of levee deposition (Figure 10c) are roughly consistent with observed levee deposits in the field (Figure 3), though this match is not perfect because our modeling is a generic representation of the Muscatatuck River.

We focus on four levee deposits that include three cut bank levee deposits (labeled 1 to 3 on Figure 10c) and one levee on a relatively straight section (labeled 4). Levees at Locations 1 and 2 are oriented approximately 45° and 30°, respectively, relative to the down-valley flow direction. Levees

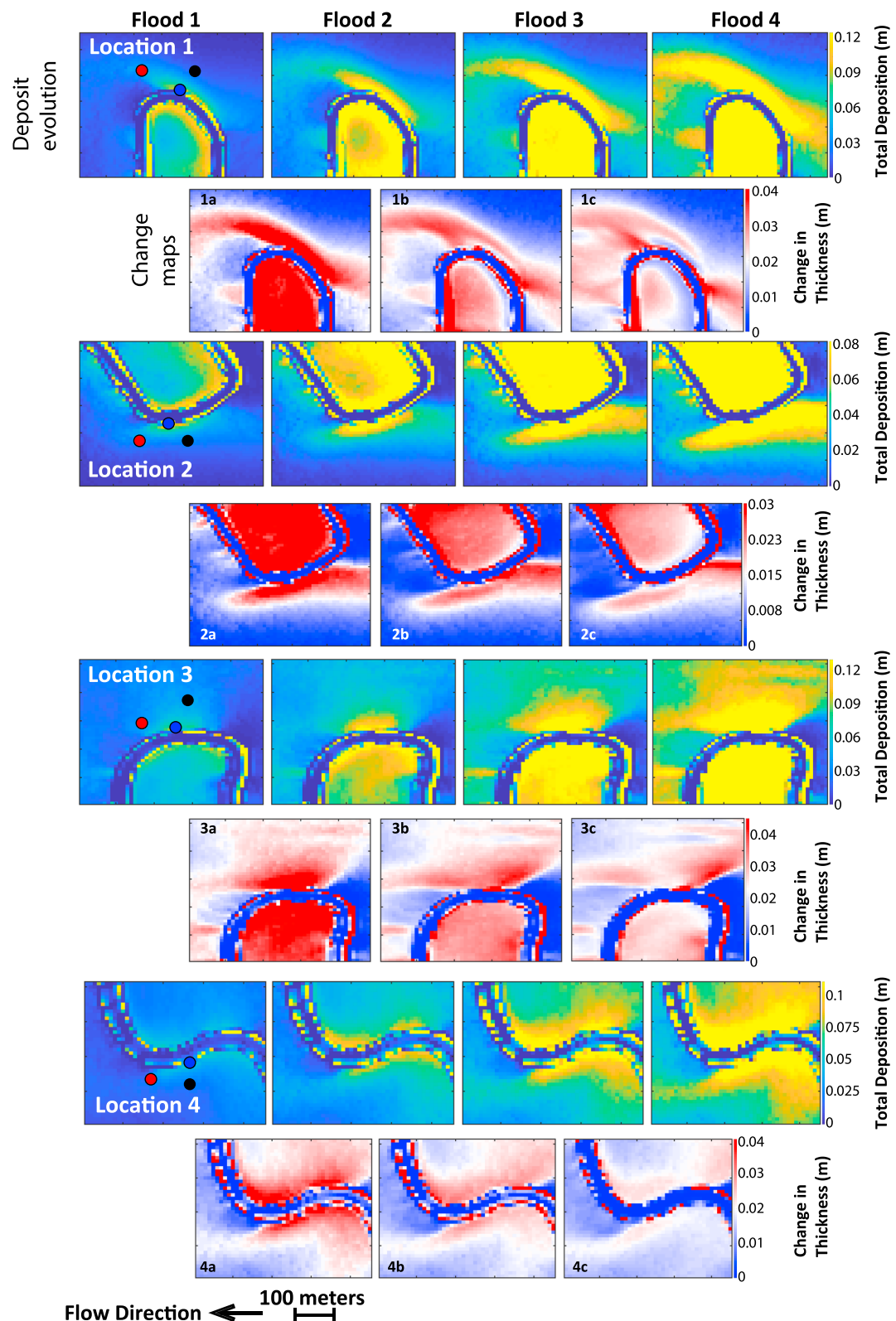


Figure 11. Model results of time evolution of levee thicknesses for Locations 1–4. For each levee, the top row shows development of the total deposit after each flood wave is complete, and the bottom row shows the change between each flood.

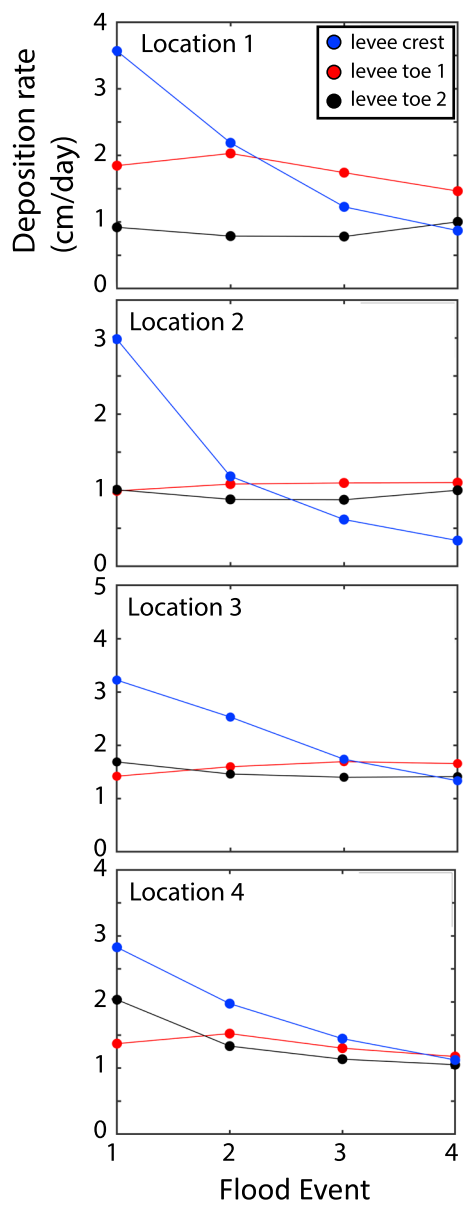


Figure 12. Deposition rate on the levee crest decreases with time, and all levees show a transition, by the fourth flood wave, where all parts of the levee grow at the same rate or the highest deposition rate is on the levee toe. Locations of deposition rate are shown with the same color dots in Figure 11.

the levee sediment was advected from the channel and immediately deposited on the margin. But this only occurs because the flood-basin hydrology and the macroroughness from the channel create a water surface gradient due to flood wave arrival time. This location illustrates that controls on levee formation can be related to channel and flood-basin conditions.

6. Discussion: What Controls Levee Size and Shape?

Given there is not strong scientific consensus on what controls levee size and shape, we started with the null hypothesis that the levee is genetically related to the adjacent channel. This could occur, for instance, if levees form in locations where floodwaters decant over the bank because the levee sediment would be directly sourced from the adjacent channel. In this case, we would expect our empirical data

(Figure 11). Down-valley progradation is especially evident for Location 1 where levee growth is oblique to the channel bank at the meander bend apex. The levee at Location 1 also widens as it grows. Levee 2 also undergoes widening and down-valley progradation. Progradation of the levee at Location 3 is less pronounced; however, this deposit also widens and begins to grow in a down-valley direction after the second flood wave. Down-valley progradation is evident along the left bank at Location 4, and both paired levees experience lateral widening.

Down-valley progradation occurs because when the levee grows, it generates a morphodynamic feedback by shifting deposition from the crest to the toe (Filgueira-Rivera et al., 2007). All levees undergo a transition from crest to toe deposition by the fourth flood waves (Figures 11 and 12). The change maps for each levee (Figure 11) show that deposition on the crest decreases from flood waves 1 to 4, while deposition on the levee toe increases or stays the same. For instance, levee deposition at Location 2 is initially at the levee crest near the channel margin (plot 2a in Figure 11), but later flood waves deposit more sediment on the leeside of the levee while sedimentation near the channel is reduced (compare plots 2b and 2c in Figure 11). The levee crest at Location 1 is subaerial through most of the fourth flood wave. This forms a bed shear stress shadow and low flow velocity zone on the leeside of the levee and leads to more deposition at the levee toe than at the crest. The transition can also be seen in the depositional rates because by the fourth flood the levee crest deposition rate is equal to or less than rate at the toe (Figure 12). This is model confirmation of the transition from front loading to back loading proposed by Filgueira-Rivera et al. (2007).

Additionally, the arrival time of the flood wave also can influence where and how levees grow. At Location 4, the channel is oriented parallel to the floodplain centerline, and levees should be built by classic mechanisms of turbulent eddy diffusion because the floodplain flow and channelized flow should be aligned (Adams et al., 2004; Pizzuto, 1987). But this site illustrates how difficult it can be to detect the controls on levee formation from this kind of reasoning alone. At Location 4, the flood wave arrives on the river right side first (Figure 10a). This sets up a water surface gradient from north to south on the river left side, which creates relatively strong flow perpendicular to the channel centerline (Figure 13a). This strong flow advects sediment from the channel into the floodplain on the river left side, and at peak discharge the gradient in sediment concentration on river left side is larger than river right (Figure 13b). Provided there is no strong cross-flow, the gradient in concentration indicates deposition. In this case, the levee is genetically connected to the channel, insofar that

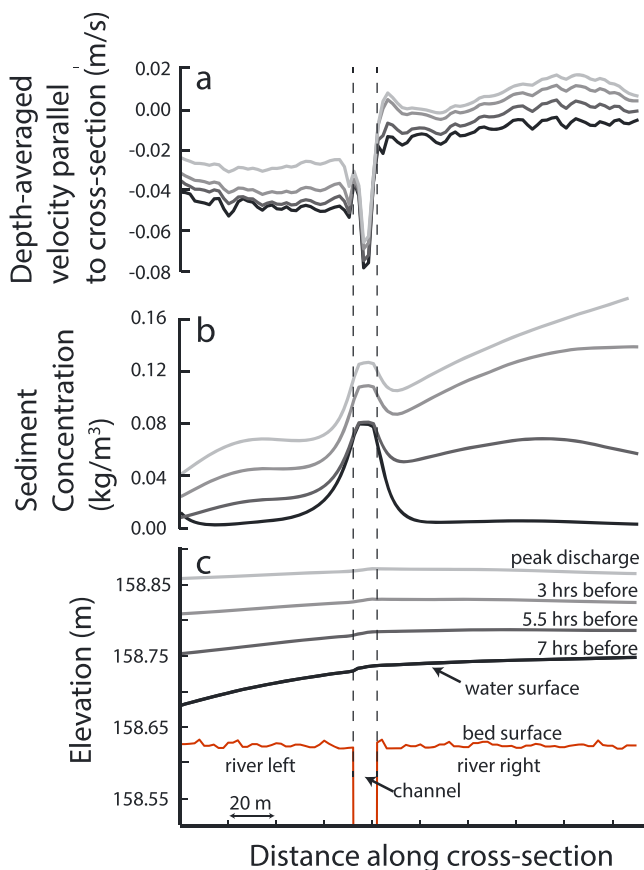


Figure 13. Time evolution of cross-section parallel flow velocity (a), sediment concentration (b), and water surface (c) at Location 4 during Flood 1. On the river left side, negative velocities in (a) correspond to a southerly flow direction, which indicates strong advective flow from the channel onto the floodplain. Near-zero velocities on the river right side mean there is little cross-section parallel flow. Cross-section location is shown on the first panel for Location 4 on Figure 11.

down the levee. But, on taller levees, flood waters flow around the levee perimeter and inundate the levee toe first.

This change in inundation pattern marks a significant transition in deposition that reshapes the levee and obscures the genetic connection to the channel. Deposition rate on smaller levees is highest on the crest because that inundates first with sediment-laden water directly from the adjacent channel (Figure 12). But the highest deposition rate on taller levees can occur at the toe because it is inundated longest with sediment-laden floodwater. This depositional transition reshapes the levee, causing it to lengthen as the toe grows faster than the crest (Filgueira-Rivera et al., 2007), and this results in levee progradation down-valley. Tall levees obstruct the propagating flood wave, creating a bed shear stress shadow on the downstream side, and sediment transported down-valley by floodplain flow is deposited within this zone of reduced flow competence (Figure 14a). Though it is difficult to say conclusively, we think some of the levees along the Muscatatuck River have morphology suggestive of down-valley progradation (Figures 14b and 14c). The modeled feedbacks between levee evolution and fluid flow suggest that after the initial levee deposition, levee morphology within fine-grained fluvial environments may be more strongly related to flood wave propagation.

We propose that the lack of relationship between the channel planform and levee size, as observed in this study, may be characteristic of fine-grained river systems in narrow floodplains. The dynamics we

from the Muscatatuck River, Indiana, USA, to show some relationship between levee size and local curvature, radii of curvature, or the angle between levee and floodplain centerlines. But this is not the case: there is no interpretable relationship between river planform and the associated levee (Figures 6–9). This is surprising because if levees form as sediment diffuses and advects from the channel to the margin (Adams et al., 2004), then advection should be enhanced where curvature is high because centripetal acceleration causes overbank flow, and advection should be enhanced in the crossover region. The crossover region is where the channel is oriented orthogonal to down-valley slope of the floodplain, and in this region, downstream-directed floodwaters would advect sediment from the channel to the margin (Sellin et al., 1993). Even in the case of Levee 4, where levee sediment is advected from the channel to the margin (Figure 13), the advection is caused by differences in floodplain arrival time at points across the floodplain, which in turn is related to inundation dynamics of the flood basin.

But the modeling suggests that levees are still connected to the morphology of the adjacent channel even though we cannot see it in the empirical data. In the modeling results, levee initiation occurs where channel curvature is high (Figure 10). This genetic connection occurs because the meandering channel acts as a macroroughness element. The channel shape creates bed shear stress shadows where curvature is high that become the sites of levee initiation (Figures 10b and 10c) and affects flood wave arrival times that set up water surface gradients to drive levee formation (Figures 10a and 13).

One reason this genetic connection may not be preserved in the empirical data is because it may be obscured on dynamic rivers. If a river frequently experiences cutoff events (Schwenk & Foufoula-Georgiou, 2016) or avulsions (Edmonds et al., 2016), levees may not adapt to local channel metrics. But this is likely not a factor for the Muscatatuck River because we see no surficial evidence of cutoff or avulsion scars in aerial images or Landsat data, which suggests the river is relatively stable. Instead, we think the lack of genetic connection occurs because as levees grow, their inundation dynamics change. Smaller levees are inundated from crest to toe as floodwaters spill out of the channel and flow

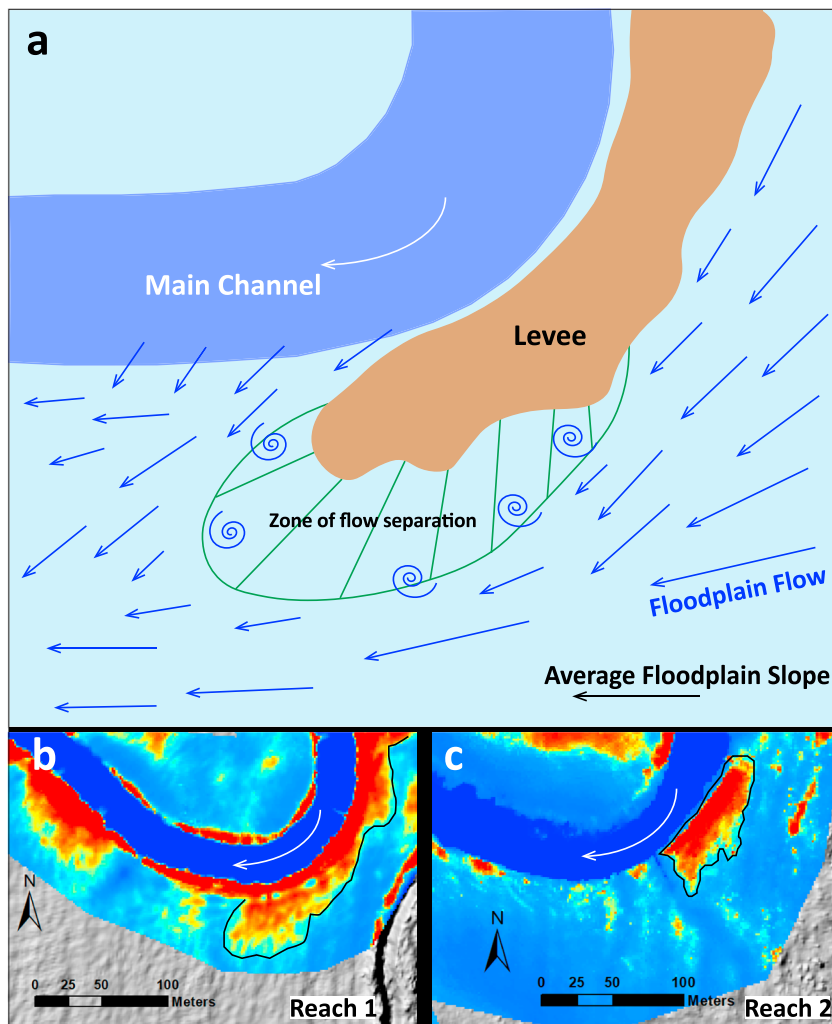


Figure 14. (a) Cartoon showing that when tall levees are not fully inundated during floods, they can create zones of flow separation. If deposition occurs in these zones it will lead to down-valley progradation. (b and c) Possible examples of levees that prograded downstream due to deposition in the zone of flow separation on Reaches 1 and 2.

see here likely apply more to narrower floodplains because they fully inundate during flood, like what we see in the model. Rivers, like the Amazon (Trigg et al., 2012), with wide floodplains may only flood part of their valley. This limits inundation and down-valley conveyance of water in the flood basin, and because of this the mechanisms we discuss in this paper may not apply to wide floodplains. Our results also probably apply to finer-grained rivers. In coarser-grained rivers, sediment rapidly falls out of suspension as fluid moves from the channel to the channel margin. If this is the only source of levee sediment, then the levees will be genetically connected to the channel. Indeed, consistent with this notion, Hudson and Heitmuller (2003) found that coarser grained levees (84th percentile of grain size ranges from 64 to 240 μm) on the coastal gulf plain rivers of Mexico are largest on the outside of meander bends. This situation may not occur on finer-grained rivers. The levees and floodplain of the Muscatatuck River have much finer sediment (84th percentile is 19–22 μm) with almost no sand-sized sediment (Figure 2b). We see no observable connection between the characteristics of the levee and the adjacent river channel, possibly because as the modeling shows, fine-grained suspended sediment is not immediately deposited when the flood wave leaves the channel. Instead, it is transported down-valley during flood, where it interacts with the channel and preexisting levee topography before it is deposited. This can decouple the levee from the adjacent channel because the growth and shape are influenced by the flood wave.

7. Conclusions

Here we tested whether levees grow and form by the transfer and deposition of sediment from the adjacent channel to the margin or by inundation dynamics in the flood basin. If levees are formed by sediment transfer from the adjacent channel, then levee size and shape should be a function of the processes that drive that transfer. Our empirical analyses show no conclusive evidence that levee presence or size is genetically related to the planform morphology of the adjacent channel. We focused on planform attributes, like the curvature of the channel and its orientation relative to the floodplain axis, because, all else being equal, a sinuous channel should transfer more sediment to the channel margins during flood.

To see why levees may not be genetically related to their adjacent channel, we conducted modeling experiments of a simplified Muscatatuck River that retains the channel planform but has a smooth floodplain. Our modeling results suggest that in fine-grained systems levee initiation is related to the channel planform. But, after levees grow tall enough relative to the flood-wave height, their crests are starved of sediment, and the deposition maximum moves to the levee toe. When this transition occurs, levees prograde down-valley, which in turn reshapes the levee and genetically disconnects it from the channel.

From these empirical and modeling results we suggest that on fine-grained rivers in narrow floodplains, levee size and shape are sensitive to flood-basin hydrology and emerge from the interactions among inundation frequency, flood wave propagation, and transport pathways of suspended sediment.

Acknowledgments

We would like to thank the donors of the American Chemical Society Petroleum Research Fund for supporting this work. We would also like to thank the Indiana University Grand Challenges *Preparing for Environmental Change* for partial support. G. J. would like to thank the American Association of Petroleum Geologists and the Society for Sedimentary Geology for providing additional research grants in support of field and laboratory work. We thank three anonymous reviewers, Associate Editor Joel Sankey, and Editor Amy East for comments that improved this manuscript. Data used in this paper are available through Indiana University's Scholar Works (<https://scholarworks.iu.edu/> and at <http://hdl.handle.net/2022/23212>).

References

- Aalto, R., Maurice-Bourgoin, L., Dunne, T., Montgomery, D. R., Nittrouer, C. A., & Guyot, J.-L. (2003). Episodic sediment accumulation on Amazonian flood plains influenced by El Niño/Southern Oscillation. *Nature*, 425(6957), 493–497. <https://doi.org/10.1038/nature02002>
- Adams, P. N., Slingerland, R. L., & Smith, N. D. (2004). Variations in natural levee morphology in anastomosed channel flood plain complexes. *Geomorphology*, 61(1–2), 127–142. <https://doi.org/10.1016/j.geomorph.2003.10.005>
- Asselman, N. E. M., & Middelkoop, H. (1995). Floodplain sedimentation—Quantities, patterns and processes. *Earth Surface Processes and Landforms*, 20(6), 481–499. <https://doi.org/10.1002/esp.3290200602>
- Brakenridge, G., Syvitski, J., Niebuhr, E., Overeem, I., Higgins, S., Kettner, A., & Prades, L. (2017). Design with nature: Causation and avoidance of catastrophic flooding, Myanmar. *Earth-Science Reviews*, 165, 81–109. <https://doi.org/10.1016/j.earscirev.2016.12.009>
- Brierley, G. J., Ferguson, R. J., & Woolfe, K. J. (1997). What is a fluvial levee? *Sedimentary Geology*, 114(1–4), 1–9. [https://doi.org/10.1016/s0037-0738\(97\)00114-0](https://doi.org/10.1016/s0037-0738(97)00114-0)
- Brooks, G. R. (2005). Overbank deposition along the concave side of the Red River meanders, Manitoba, and its geomorphic significance. *Earth Surface Processes and Landforms*, 30(13), 1617–1632. <https://doi.org/10.1002/esp.1219>
- Bryant, M., Falk, P., & Paola, C. (1995). Experimental study of avulsion frequency and rate of deposition. *Geology*, 23(4), 365–368. [https://doi.org/10.1130/0091-7613\(1995\)023<0365:ESOAFA>2.3.CO;2](https://doi.org/10.1130/0091-7613(1995)023<0365:ESOAFA>2.3.CO;2)
- Cazanacli, D., & Smith, N. D. (1998). A study of morphology and texture of natural levees—Cumberland Marshes, Saskatchewan, Canada. *Geomorphology*, 25(1–2), 43–55. [https://doi.org/10.1016/S0169-555X\(98\)00032-4](https://doi.org/10.1016/S0169-555X(98)00032-4)
- Clark, L., & Wynn, T. (2007). Methods for determining streambank critical shear stress and soil erodibility: Implications for erosion rate predictions. *Transactions of the ASABE*, 50(1), 95–106. <https://doi.org/10.13031/2013.22415>
- Czuba, J. A., David, S. R., Edmonds, D. A., & Ward, A. S. (2019). Dynamics of surface-water connectivity in a low-gradient meandering river floodplain. *Water Resources Research*, 55, 1849–1870. <https://doi.org/10.1029/2018WR023527>
- David, S. R., Edmonds, D. A., & Letsinger, S. L. (2017). Controls on the occurrence and prevalence of floodplain channels in meandering rivers. *Earth Surface Processes and Landforms*, 42, 460–472. <https://doi.org/10.1002/esp.4002>
- Edmonds, D. A., Hajek, E. A., Downton, N., & Bryk, A. B. (2016). Avulsion flow-path selection on rivers in foreland basins. *Geology*, 44(9), 695–698. <https://doi.org/10.1130/G38082.1>
- Edwards, T. K., Glysson, G. D., Guy, H. P., & Norman, V. W. (1999). *Field methods for measurement of fluvial sediment*. Denver, CO: US Geological Survey.
- Ervine, D. A., Babaeyan-Koopaei, K., & Sellin, R. H. (2000). Two-dimensional solution for straight and meandering overbank flows. *Journal of Hydraulic Engineering*, 126(9), 653–669. [https://doi.org/10.1061/\(ASCE\)0733-9429\(2000\)126:9\(653\)](https://doi.org/10.1061/(ASCE)0733-9429(2000)126:9(653))
- Ervine, D. A., Willetts, B. B., Sellin, R. H. J., & Lorena, M. (1993). Factors affecting conveyance in meandering compound flows. *Journal of Hydraulic Engineering*, 119(12), 1383–1399. [https://doi.org/10.1061/\(ASCE\)0733-9429\(1993\)119:12\(1383\)](https://doi.org/10.1061/(ASCE)0733-9429(1993)119:12(1383))
- Ferguson, R., & Church, M. (2004). A simple universal equation for grain settling velocity. *Journal of Sedimentary Research*, 74(6), 933–937. <https://doi.org/10.1306/051204740933>
- Ferguson, R. J., & Brierley, G. J. (1999). Levee morphology and sedimentology along the lower Tuross River, South-Eastern Australia. *Sedimentology*, 46(4), 627–648. <https://doi.org/10.1046/j.1365-3091.1999.00235.x>
- Fielding, C. R., & Crane, R. C. (1987). An application of statistical modelling to the prediction of hydrocarbon recovery factors in fluvial reservoir sequences. In F. G. Ethridge, R. M. Flores, & D. Harvey (Eds.), *Recent developments in fluvial sedimentology, SEPM Special Publication* (Vol. 39, pp. 321–327). <https://doi.org/10.2110/pec.87.39.0321>
- Filgueira-Rivera, M., Smith, N. D., & Slingerland, R. L. (2007). Controls on natural levee development in the Columbia River, British Columbia, Canada. *Sedimentology*, 54(4), 905–919. <https://doi.org/10.1111/j.1365-3091.2007.00865.x>
- Hudson, P. F., & Heitmuller, F. T. (2003). Local- and watershed-scale controls on the spatial variability of natural levee deposits in a large fine-grained floodplain: Lower Panuco Basin, Mexico. *Geomorphology*, 56(3–4), 255–269. [https://doi.org/10.1016/s0169-555x\(03\)00155-7](https://doi.org/10.1016/s0169-555x(03)00155-7)
- Hum, Y. C., Lai, K. W., & Mohamad Salim, M. I. (2014). Multiobjectives bihistogram equalization for image contrast enhancement. *Complexity*, 20(2), 22–36. <https://doi.org/10.1002/cplx.21499>

- Iseya, F., & Ikeda, H. (1989). *Sedimentation in coarse-grained sand-bedded meanders: Distinctive deposition of suspended sediment*. Tokyo: Terra Scientific Publishing (TERRAPUB).
- James, C. S. (1985). Sediment transfer to overbank sections. *Journal of Hydraulic Research*, 23(5), 435–452. <https://doi.org/10.1080/00221688509499337>
- Kesel, R. H., Dunne, K. C., McDonald, R. C., Allison, K. R., & Spicer, B. E. (1974). Lateral erosion and overbank deposition on the Mississippi River in Louisiana caused by 1973 flooding. *Geology*, 1, 461–464.
- Kimiaghalam, N., Clark, S. P., & Ahmari, H. (2016). An experimental study on the effects of physical, mechanical, and electrochemical properties of natural cohesive soils on critical shear stress and erosion rate. *International Journal of Sediment Research*, 31(1), 1–15. <https://doi.org/10.1016/j.ijsrc.2015.01.001>
- Lesser, G., Roelvink, J., van Kester, J., & Stelling, G. (2004). Development and validation of a three-dimensional morphological model. *Coastal Engineering*, 51, 883–915.
- Maa, J. P. Y., Kwon, J. I., Hwang, K. N., & Ha, H. K. (2008). Critical bed-shear stress for cohesive sediment deposition under steady flows. *Journal of Hydraulic Engineering-ASCE*, 134(12), 1767–1771. [https://doi.org/10.1061/\(ASCE\)0733-9429\(2008\)134:12\(1767\)](https://doi.org/10.1061/(ASCE)0733-9429(2008)134:12(1767))
- Mackey, S. D., & Bridge, J. S. (1995). Three-dimensional model of alluvial stratigraphy: Theory and application. *Journal of Sedimentary Research*, 65(1b), 7–31. <https://doi.org/10.1306/D42681D5-2B26-11D7-8648000102C1865D>
- Marriott, S. (1992). Textural analysis and modelling of a flood deposit: River Severn, U.K. *Earth Surface Processes and Landforms*, 17(7), 687–697. <https://doi.org/10.1002/esp.3290170705>
- Mertes, L. A. K. (1997). Documentation and significance of the perirheic zone on inundated floodplains. *Water Resources Research*, 33(7), 1749–1762. <https://doi.org/10.1029/97WR00658>
- Middelkoop, H., & van der Perk, M. (1998). Modelling spatial patterns of overbank sedimentation on embanked floodplains. *Geografiska Annaler Series A-Physical Geography*, 80(2), 95–109. <https://doi.org/10.1111/j.0435-3676.1998.00029.x>
- Mohrig, D., Heller, P. L., Paola, C., & Lyons, W. J. (2000). Interpreting avulsion process from ancient alluvial sequences: Guadalupe-Matarranya system (northern Spain) and Wasatch Formation (western Colorado). *Geological Society of America Bulletin*, 112(12), 1787. [https://doi.org/10.1130/0016-7606\(2000\)112<1787:IAPFAA>2.0.CO;2](https://doi.org/10.1130/0016-7606(2000)112<1787:IAPFAA>2.0.CO;2)
- Nanson, G., & Croke, J. (1992). A genetic classification of floodplains. *Geomorphology*, 4(6), 459–486. [https://doi.org/10.1016/0169-555X\(92\)90039-Q](https://doi.org/10.1016/0169-555X(92)90039-Q)
- Nezu, I., & Nakagawa, H. (1993). *Turbulence in open-channel flows*, (p. 281). Rotterdam Brookfield: A.A. Balkema.
- Nicholas, A. P., & Mitchell, C. A. (2003). Numerical simulation of overbank processes in topographically complex floodplain environments. *Hydrological Processes*, 17(4), 727–746. <https://doi.org/10.1002/hyp.1162>
- Pierik, H., Stouthamer, E., & Cohen, K. (2017). Natural levee evolution in the Rhine-Meuse delta, the Netherlands, during the first millennium CE. *Geomorphology*, 295, 215–234. <https://doi.org/10.1016/j.geomorph.2017.07.003>
- Pizzuto, J. E. (1987). Sediment diffusion during overbank flows. *Sedimentology*, 34(2), 301–317. <https://doi.org/10.1111/j.1365-3091.1987.tb00779.x>
- Pizzuto, J. E., Moody, J. A., & Meade, R. H. (2008). Anatomy and dynamics of a floodplain, Powder River, Montana, USA. *Journal of Sedimentary Research*, 78(1), 16–28. <https://doi.org/10.2110/jsr.2008.005>
- Ranasinghe, R., Swinkels, C., Luijendijk, A., Roelvink, D., Bosboom, J., Stive, M., & Walstra, D. J. (2011). Morphodynamic upscaling with the MORFAC approach: Dependencies and sensitivities. *Coastal Engineering*, 58, 806–811.
- Roelvink, J. (2006). Coastal morphodynamic evolution techniques. *Coastal Engineering*, 53(2–3), 277–287. <https://doi.org/10.1016/j.coastaleng.2005.10.015>
- Schwenk, J., & Foufoula-Georgiou, E. (2016). Meander cutoffs nonlocally accelerate upstream and downstream migration and channel widening. *Geophysical Research Letters*, 43, 12,437–12,445. <https://doi.org/10.1002/2016GL071670>
- Schwenk, J., Khandelwal, A., Fratkin, M., Kumar, V., & Foufoula-Georgiou, E. (2017). High spatiotemporal resolution of river planform dynamics from Landsat: The RivMAP toolbox and results from the Ucayali River. *Earth and Space Science*, 4, 46–75. <https://doi.org/10.1002/2016EA000196>
- Sellin, R. H. J., Ervine, D. A., & Willetts, B. B. (1993). Behavoir of meandering two-stage channels. *Proceedings of the Institution of Civil Engineers - Water, Maritime and Energy*, 101(2), 99–111. <https://doi.org/10.1680/iwtme.1993.23591>
- Shiono, K., & Knight, D. W. (1991). Turbulent open-channel flows with variable depth across the channel. *Journal of Fluid Mechanics*, 222(1), 617–646. <https://doi.org/10.1017/S0022112091001246>
- Shiono, K., & Muto, Y. (1998). Complex flow mechanisms in compound meandering channels with overbank flow. *Journal of Fluid Mechanics*, 376, 221–261.
- Simmons, K. (2014). *Sediment samples (operating procedure No. SESDPROC-200-R3)*. United States Environmental Protection Agency, Region 4.
- Smith, N. D., Cross, T. A., Dufficy, J. P., & Clough, S. R. (1989). Anatomy of an avulsion. *Sedimentology*, 36(1), 1–23. <https://doi.org/10.1111/j.1365-3091.1989.tb00817.x>
- Smith, N. D., Pérez-Arlucea, M., Edmonds, D. A., & Slingerland, R. L. (2009). Elevation adjustments of paired natural levees during flooding of the Saskatchewan River. *Earth Surface Processes and Landforms*, 34(8), 1060–1068. <https://doi.org/10.1002/esp.1792>
- Trigg, M. A., Bates, P. D., Wilson, M. D., Schumann, G., & Baugh, C. (2012). Floodplain channel morphology and networks of the middle Amazon River. *Water Resources Research*, 48, W10504. <https://doi.org/10.1029/2012WR011888>
- Vargas-Luna, A., Crosato, A., Anders, N., Hoitink, A. J., Keesstra, S. D., & Uijttewaal, W. S. (2018). Morphodynamic effects of riparian vegetation growth after stream restoration. *Earth Surface Processes and Landforms*, 43(8), 1591–1607. <https://doi.org/10.1002/esp.4338>
- Walling, D., & He, Q. (1998). The spatial variability of overbank sedimentation on river floodplains. *Geomorphology*, 24(2–3), 209–223. [https://doi.org/10.1016/S0169-555X\(98\)00017-8](https://doi.org/10.1016/S0169-555X(98)00017-8)
- Wolpert, H., Hommel, P., Prins, A., & Stam, M. (2002). The formation of natural levees as a disturbance process significant to the conservation of riverine pastures. *Landscape Ecology*, 17(1suppl), 47–57. <https://doi.org/10.1023/A:1015229710294>